Optical and morphological characterization of TiO_2 films doped with silver nanoparticles

G. Valverde-Aguilar[1*], J. A. García-Macedo [1], V. Renteria-Tapia[1]

1. Departamento de Estado Sólido. Instituto de Física, Universidad Nacional Autónoma de México. México D.F. C.P. 04510. Tel. (5255) 5622–51–03, Fax (5255) 616–15–35. E–mail: valverde@fisica.unam.mx

*** Contact author:**
Dr. Jorge Garcia Macedo
Instituto de Física, UNAM
Circuito de la Inv. Científica s/n
C. P. 04510. Del. Coyoacán
México, D.F.
México.
Tel. (5255) 5622–51–03
Fax (5255) 5616–15–35
E–mail: gamaj@fisica.unam.mx

ABSTRACT

Silver-doped titanium dioxide thin films were deposited on glass substrates by the sol–gel process. Undoped films and films doped with 1 mol% $AgNO_3$ were annealed at 100°C for 30 minutes and sintered at 520°C for 1 hour. The optical and morphological properties of the films were analyzed by optical absorption spectroscopy, X-ray diffraction and scanning electron microscopy. Two crystalline phases, anatase and rutile were identified in the films by X-ray diffraction. An absorption band was located at 415 nm which is associated to the surface plasmon resonance of the silver nanoparticles. This spectrum was modelled using the Gans theory considering small silver nanoparticles with diameters of 3 nm and a refractive index lower than that coming from host matrix.

KEYWORDS: Titania, silver nanoparticles, sol-gel, thin film, spin-coating, Gans theory, refractive index

1. INTRODUCTION

Noble metal nanoparticles and especially silver nanoparticles exhibit an absorption band in the visible region caused by the surface plasmon resonance (SPR); as well-known the SPR wavelength and intensity depend on the nanoparticle size, geometry and environment (dielectric constant and interparticle distance).[1-3]

Titanium dioxide (TiO_2) has attracted significant attention of researchers because of many interesting physical properties that make it suitable for a variety of applications, for example, TiO_2 has high corrosion resistance, chemical stability, and an excellent optical transparency in the visible and near infrared regions as well as high refractive index that makes it useful for antireflection coatings in optical devices.

In this paper, we were interested in the synthesis and characterization of crystalline TiO_2 films doped with silver nanoparticles (NPs). The films were produced by the sol–gel process at room temperature. The films were deposited on glass wafers by the spin-coating method. Silver NPs have been produced into the titania matrix by sinterization treatment at 520°C for 1 hour. The optical absorption (OA) spectrum was modelled using the Gans theory. The position of the surface plasmon resonance (SPR) was studied.

Plasmonics: Metallic Nanostructures and Their Optical Properties VIII, edited by Mark I. Stockman,
Proc. of SPIE Vol. 7757, 77572Z · © 2010 SPIE · CCC code: 0277-786X/10/$18 · doi: 10.1117/12.860612

The obtained films were characterized by X-ray diffraction (XRD), infrared spectroscopy (IR) and scanning electron microscopy (SEM) studies too.

2. EXPERIMENTAL

Glass substrates were cleaned in boiling acidic solution of sulphuric acid-H_2O_2 (4:1) under vigorous stirring for 30 minutes. They were then placed in deionized water and boiled for 30 minutes, rinsed three times with deionized water and stored in deionized water at room temperature.

Preparation of TiO_2 solution. First, the precursor solutions for TiO_2 films were prepared by the following method. Tetrabutyl orthotitanate and diethanolamine ($NH(C_2H_4OH)_2$) which prevent the precipitation of oxides and stabilize the solutions were dissolved in ethanol. After stirring vigorously for 2h at room temperature, a mixed solution of deionized water and ethanol was added dropwise slowly to the above solution with a pipette under stirring. Finally, Tetraethyleneglycol (TEG) was added to the above solution. This solution was stirred vigorously to obtain an uniform sol. The resultant alkoxide solution was kept standing at room temperature to perform hydrolysis reaction for 2h, resulting in the TiO_2 sol. The final chemical composition of this solution was $Ti(OC_4H_9)_4$: $NH(C_2H_4OH)_2$: C_2H_5OH : DI H_2O : TEG: nitric acid: $AgNO_3$ = 1:1: 14.1:1:1.028:0.136.

Second, 4g of DI H_2O, 0.3 g nitric acid and 0.047 M of $AgNO_3$ salt were added to 21.6 ml of TiO_2 solution. It was stirred for 4 hours at room temperature. The TiO_2 with silver NPs solution has a pH = 6.0. The TiO_2 and TiO_2/Ag films were prepared by the spin-coating technique. The precursor solution was placed on the glass wafers (2.5 x 2.5 cm^2) using a dropper and spun at a rate of 4000 rpm for 15 s (Figure 1).

Figura 1. Spin-coating technique.

After coating, the film was dried at 100 °C for 30 min in a muffle oven and sintered at 520 °C for 1 h in the same muffle in order to remove organic components. The procedure was repeated two times to achieve the film thickness with three layers. The films show a brown colour.

UV-vis absorption spectra were obtained on a Thermo Spectronic Genesys 2 spectrophotometer with an accuracy of ±1 nm over the wavelength range of 300-900 nm. The structure of the final films was characterized by XRD patterns. These patterns were recorded on a Bruker AXS D8 Advance diffractometer using Ni-filtered CuKα radiation. A step-scanning mode with a step of 0.02° in the range from 1.5 to 60° in 2θ and an integration time of 2 s was used. FTIR spectra were obtained from a KBr pellet using a Bruker Tensor 27 FT-IR spectrometer. Pellets were made from a finely ground mixture of the sample and KBr at a ratio of KBr:sample = 1:6 x 10^{-4}. The thickness of the films was measured using a SEM microscopy Model STEREOSCAN at 20 kV.

3. RESULTS AND DISCUSSION

3.1 X-ray diffraction patterns. The X-ray diffraction pattern at high angle of amorphous and crystalline TiO_2 films with silver NPs are shown in Figure 2. Amorphous films did not exhibit any peak in its pattern. The films sintered at 520 °C for 1 hour exhibit a good crystallization that corresponds to anatase and rutile phases. The anatase phase was identified by the diffraction peaks located at 2θ =25.33, 37.74, 38.02 and 48.02 which can be indexed as (101), (004), (112) and (200) respectively. The rutile phase was identified by the diffraction peaks located at 2θ = 27.47, 36.11, 41.29, 44.13 and 54.40 which can be indexed as (110), (101), (111), (210) and (211) respectively. The position of the diffraction peaks in the film is in good agreement with those given in ASTM data card (#21-1272) for anatase and ASTM data card (#21-1276) for rutile.

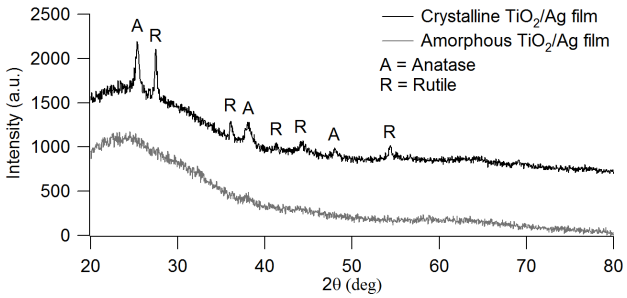

Figure 2. X-ray diffraction patterns at high angle of amorphous TiO_2/Ag film (grey solid line) and crystalline TiO_2/Ag film sintered at 520 °C for 1 hour (black solid line).

The average crystalline size (D) was calculated from Scherrer´s formula [4] by using the diffraction peak (101) for anatase phase and the peak (110) for rutile phase:

$$D = \frac{0.9\lambda}{B\cos\theta} \qquad (1)$$

with λ=1.54056x10^{-10} m. Table 1 contains the results.

The weight fractions of rutile (x_r) and anatase (x_a) present in the film samples can be calculated by the following equations respectively [5]:

$$x_r = \frac{I_r}{0.884I_a + I_r}, \qquad x_a = \frac{0.884I_a}{0.884I_a + I_r} \qquad (2)$$

where I_r and I_a are the integrated intensities of rutile (110) and anatase (101) peaks. These calculations are shown in Table 1. Anatase is the dominant phase in the films with 60.8 wt%, while the rutile is only the 39.2 wt%.

Table 1. Summary of nanoscopic characteristics of crystalline TiO_2/Ag film.

Phase	B	Radian	D (nm)	Crystal phase (wt%)
Anatase (101)	0.4545°	0.0079	18	60.8
Rutile (110)	0.25°	0.00436	33	39.2

3.2 Optical absorption. Figure 3 shows the optical absorption spectra of amorphous and crystalline TiO_2 films with and without silver NPs taken at room temperature in the range of 270-900 nm. For crystalline TiO_2 film, its spectrum shows an absorption band A located at 319 (3.89 eV) corresponding to the TiO_2 matrix. For crystalline TiO_2/Ag film an absorption band B is located 415 nm (2.99 eV) corresponding to the surface plasmon resonance (SPR) of the silver NPs. For amorphous TiO_2/Ag film any band was observed. The absorption peak located at short wavelength for amorphous TiO_2/Ag film and crystalline TiO_2 film indicates the presence of un-burned organic residuals remaining in the films. As observed in the spectrum for crystalline TiO_2/Ag film, such organic residuals are removed by increasing the annealing temperature to 520 °C.

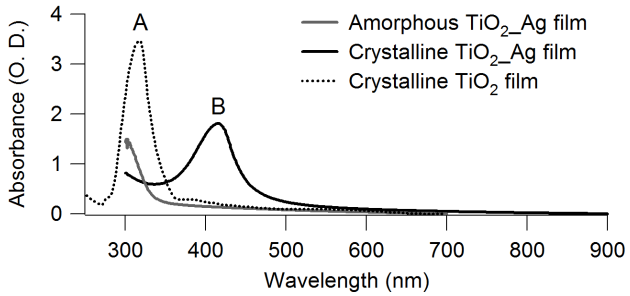

Figure 3. Absorption spectra of: (a) amorphous TiO_2/Ag film (grey solid line), (b) crystalline TiO_2/Ag film (black solid line) and (c) crystalline TiO_2 film (black dotted line).

The OA spectra of TiO_2/Ag film calcined at 100, 200, 500 and 600 °C for 1 h is shown in Figure 4. The films calcined at 100 and 200 °C did not show any crystallization. They exhibit a broad band in their absorption spectrum, it means that the NPs are too big and deformed, and the presence of un-burned organic residuals remaining in the films.

On the contrary, the crystalline films calcined at 500 and 600 °C exhibit a narrow and well defined optical spectrum which means that the silver NPs are very small and almost spherical.

Therefore, the plasmonic band shows a large UV-shift in the range from 540 to 406 nm. This shift is claimed to be related to the size of silver NPs or to the interaction between TiO_2 and Ag [6].

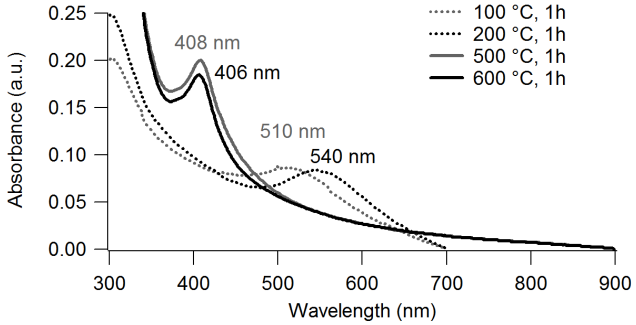

Figure 4. OA spectra of TiO_2/Ag film calcined at 100 °C (dotted grey line), 200 °C (dotted black line), 500 °C (solid grey line) and 600 °C (solid black line) for 1 h.

The optical band-gap, Eg, was determined from the absorption spectra (Figure 3) using equation [7, 8]:

$$(\alpha h\nu)^2 = C(h\nu - E_g) \qquad (1)$$

where α is the absorption coefficient, $h\nu$ is the photon energy, E_g is the band gap energy and C depends on the electron-hole mobility.

Table 2 contains the E_g values for TiO_2, amorphous TiO_2/Ag and crystalline TiO_2/Ag calculated by using the eq. (1). These values are similar to those reported by S.A. Tomás *et al.* [9] treated in similar conditions as our samples.

Table 2. Band gap values.

Sample	Literature (eV) (Ref. 8)	Calculated (eV)
TiO_2	3.61	3.68
Amorphous TiO_2/Ag	3.53	3.54
Crystalline TiO_2/Ag	3.45	3.41
Anatase	3.20	-
Rutile	3.00	-

Eg varied from 3.68 eV for crystalline TiO_2 to 3.54 eV for amorphous TiO_2/Ag films. At 520 °C, the sample has a band-gap energy close to 3.41 eV. All these values are higher than those reported for anatase (3.2 eV) and rutile (3.0 eV) TiO_2 and are attributed to thermal stress effects produced in the film [10].

After annealing at 520 °C for 1 h, the crystalline TiO_2/Ag film exhibited an absorption peak centered at 415 nm associated with the typical surface plasmon absorption of Ag nanoparticles [11]. This absorption feature has been previously reported for TiO_2/Ag films synthesized by sol–gel and other chemical methods, each by different routes.[10, 11]

The optical absorption spectrum (Fig. 3) was fitted very well using Gans theory [12] with a local refractive index n_{local} = 1.6 (Figure 5). This index is a high value, but it is not close to the refractive index reported for the anatase phase ($n_{anatase}$ = 2.54) [13] or rutile phase (n_{rutile} = 2.75) [13]. Then, the refractive index did not play an important role. [6] The diameter of the silver NPs should be between 2-5 nm and these NPs have an almost spherical shape according to the parameters used in the theoretical fit.

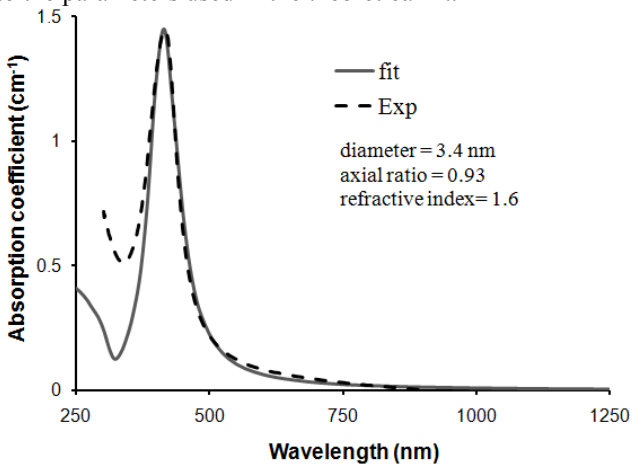

Figure 5. Experimental OA spectrum for crystalline TiO_2/Ag film (black dotted line). The calculated optical absorption spectrum (grey solid line) obtained by Gans theory.

3.3 IR spectroscopy. Figure 6 shows IR spectrum of crystalline TiO_2/Ag film prepared as KBr pellet. The bands located at 399.5 cm^{-1}, 516.9 and 646.1 cm^{-1} correspond to the anatase phase [14]. For rutile phase, the bands correspond to those located at 451.3 cm-1 and 619.1 cm^{-1}. [14]

The strong bands centered at 1247.9 and 1097.5 cm^{-1} originate in the C-O-C bonds of TEG [16]. Table 3 contains the bands of crystalline TiO_2 sample and their description.

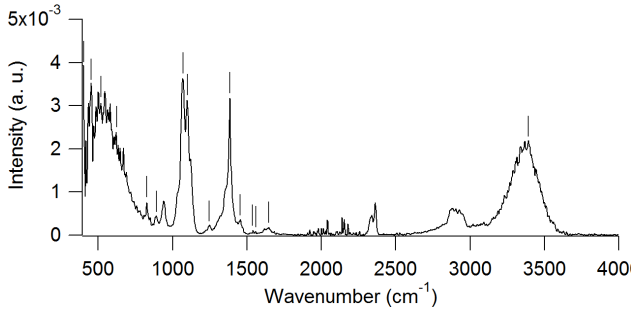

Figure 6. FTIR spectrum of crystalline TiO_2 film with silver NPs annealed at 520 °C for 1 hour. The sample was prepared as KBr pellet.

Table 3. IR frequencies [in cm^{-1}] of the crystalline TiO_2/Ag film.

Crystalline TiO_2/Ag		
ν_{exp} (cm^{-1})	description	Ref.
399.3	Anatase	14
451.3	Rutile	14
516.9	Anatase	14
619.1	Rutile	14
646.1	Anatase	14
825.5	TEG	Aldrich
891.1	TEG	Aldrich
1068.5	EtOH	15
1097.5	C-O-C bond of TEG	16
1247.9	C-O-C bond of TEG	16
1384.8	-	-
1456.2	asymm. scissoring	16
1541.1	-	-
1558.4	-	-
1647.1	ν_{OH}	16
1683.8	C=C stretching	17
3394.6	OH stretching	18

3.4 SEM measurements. The thickness of the films was measured by SEM technique. Figure 7 shows the SEM image for crystalline TiO_2 film with silver NPs, the thickness is 2.4 ± 0.4 μm.

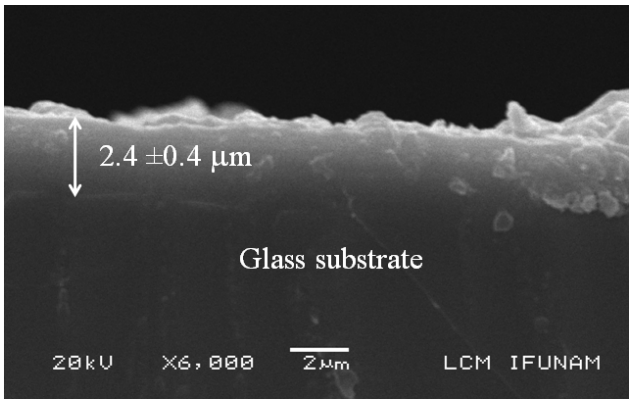

Figure 7. Cross-sectional SEM image of crystalline TiO_2/Ag film.

4. CONCLUSIONS

Undoped and Ag-doped TiO_2 films were prepared by the sol–gel process and analyzed at different annealing temperatures. The size and shape of the silver NPs modifies the position of the SPR in the optical absorption spectra. For TiO_2/Ag films without crystallization, the SPR was located around at 540 nm, while the crystalline films calcined at 500, 520 and 600 °C, the SPR was located around at 406 nm (UV region). This fact corresponds to a change from big and deformed NPs to very small and spherical ones. This large UV-shift of the

plasmonic band in the range from 540 to 406 nm is related to the size of silver NPs and/or to the interaction between TiO_2 and Ag. Small size agrees with the values obtained in the theoretical fit of the optical absorption spectrum from crystalline TiO_2/Ag.

ACKNOWLEDGMENTS

The authors acknowledge the financial supports of CONACYT 79781, NSF-CONACYT, PUNTA, ICYTDF and PAPIIT IN107510. GVA is grateful for CONACYT support. We thank to Sci. M. in Sci. Manuel Aguilar-Franco (XRD), Jaqueline Cañetas-Ortega (SEM) and Diego Quiterio (preparation of samples for SEM) for technical assistance.

REFERENCES

[1] El-Sayed, M. A., "Some Interesting Properties of Metals Confined in Time and Nanometer Space of Different Shapes", Acc. Chem. Res. 34(4), 257–264 (2001).
[2] Faraday, M., "Experimental Relations of Gold (and Other Metals) to Light", Philos. Trans. R. Soc. 147, 145-181 (1857).
[3] Mulvaney, P., "Surface Plasmon Spectroscopy of Nanosized Metal Particles", Langmuir 12, 788–800 (1996).
[4] Wilson, G. J., Matijasevich, A. S., G. Mitchell, D. R., Schulz, J. C., Will, G. D., "Modification of TiO_2 for Enhanced Surface Properties: Finite Ostwald Ripening by a Microwave Hydrothermal Process", Langmuir 22(5), 2016-2027 (2006).
[5] Chen, W., Geng, Y., Sun, X.-D., Cai, Q., Li, H.-D., Weng, D., "Achievement of thick mesoporous TiO_2 crystalline films by one-step dip-coating approach", Microporous and Mesoporous Materials 111, 219–227 (2008).
[6] He, J., Ichinose, I., Kunitake, T., Nakao, A., "In Situ Synthesis of Noble Metal Nanoparticles in Ultrathin TiO2−Gel Films by a Combination of Ion-Exchange and Reduction Processes", Langmuir 18, 10005-10010 (2002).
[7] Tauc, J., Grigorovichi, R., Vancu, A., "Optical properties and electronic structure of amorphous germanium", Phys. Status Solidi. 15, 627–633 (1966).
[8] Valle, G. G., Hammer, P., Pulcinelli, S. H., Santilli, C. V., "Transparent and conductive ZnO:Al thin films prepared by sol-gel dip-coating", Journal of the European Ceramic Society 24(6), 1009–1013 (2004).
[9] Tomás, S.A., Luna-Resendis, A., Cortés-Cuautli, L.C., Jacinto, D., "Optical and morphological characterization of photocatalytic TiO_2 thin films doped with silver", Thin Solid Films 518, 1337–1340 (2009).
[10] Yu, J., Xiong, J., Cheng, B., Liu, S., "Fabrication and characterization of Ag–TiO_2 multiphase nanocomposite thin films with enhanced photocatalytic activity", Appl. Catal. B 60, 211-221 (2005).
[11] Stathatos, E., Lianos, P., Falaras, P., Siokou, A., "Photocatalytically Deposited Silver Nanoparticles on Mesoporous TiO_2 Films", Langmuir 16, 2398-2400 (2000).
[12] Rentería, V. M., García–Macedo, J., "Influence of the local dielectric constant on modeling the optical absorption of silver nanoparticles in silica gels", Colloids and Surfaces A: Physicochemical and Engineering Aspects, 278, 1-9 (2006).
[13] Wang, Z., Helmersson, U., Käll, P.-O., "Optical properties of anatase TiO_2 thin films prepared by aqueous sol–gel process at low temperature", Thin Solid Films 405, 50–54 (2002).
[14] Jackson, K., "A Guide to Identifying Common Inorganic Fillers and Activators using Vibrational Spectroscopy", John Wiley &Sons, Ltd. (2004).
[15] Plyler, E. K., "Infrared spectra of Methanol. Ethanol, and *n*-Propanol", J. Res. of the Net. Bureau of Standards 48 (4), 281-286 (1952).
[16] Djaoued, Y., Badilescu, S., Ashrit, P. V., "Low Temperature Sol-Gel Preparation of Nanocrystalline TiO_2 Thin Films", J. Sol-Gel Sci. & Techn. 24(3), 247–254 (2002).
[17] Chiu, W.-M., Yang, C.-F., Chao, Y.-H., "Synthesis and Characterization of Titanium Dioxide Optical Films by Sol–Gel Processes", J. Appl. Polym. Sci. 103, 2271-2280 (2007).
[18] Jacyna-Onyszkiewicz, I., Grunwald-Wyspianska, M., Kaczmarek, W. A., "IR Studies of the Phase Transformation of $Fe_2O_3 \rightarrow Fe_3O_4$ by Magnetomechanical Activation", J. Phys. IV France 7, C1-615 to C1-616 (1997).